Eur. Phys. J. Appl. Phys. **82**, 30501 (2018)

https://doi.org/10.1051/epjap/2018180115

THE EUROPEAN PHYSICAL JOURNAL APPLIED PHYSICS

Regular Article

Effect of noise on measurements of diffusivity in transparent liquid mixtures by digital speckle photography

Cinzia De Leo*, Domenica Paoletti, and Dario Ambrosini

DIIIE, University of L'Aquila, P.le Pontieri 1, 67040 L'Aquila, Italy

Received: 6 April 2018 / Received in final form: 14 July 2018 / Accepted: 16 July 2018

Abstract. Interfacing two liquid mixtures in a diffusion cell induces noise in the initial state of the diffusing system, which produces a gap between the diffusion boundary and the ideally boundary assumed in the theory. Measured diffusivity values systematically drift with time and they are often corrected by using a linear shift of the zero-time of the process after sufficiently long time when the system reaches the free one-dimensional diffusion regime. In data analysis methods which involve optical correlation between pairs of successive digital images of the cell, it is not easy to establish how long the transient lasts. We show that when the initial perturbation between solution and solvent relaxes slowly toward the diffusive regime no simple zero-time correction can be applied.

1 Introduction

Diffusion is a molecular mass transport process which in transparent media can be suitably studied by optical imaging techniques which have a long tradition in visualization and in flow analysis since they are sensitive and non destructive investigation techniques. A standard optical method for measuring the diffusion coefficient in liquid binary mixtures is that of observing a free one-dimensional diffusion process: a sharp concentration gradient is first set up between two liquids, solution and solvent. The decay of the gradient is then observed illuminating the cell with a laser light beam in a direction perpendicular to the gradient. The dynamics of the decaying process is described by Fick's second law of diffusion with the initial condition referring to the Heaviside step function for the concentration distribution. A measurement of the time evolution of the refractive index or of the refractive index gradient profile gives an estimate of the mass diffusion coefficient [1].

Different experimental methods have been developed to form an initial sharp diffusion boundary, such as by using a diaphragm cell [2], the critical temperature to make fluids in two initial immiscible phases [3] or fluid injection procedures controlled by capillary tubes [4]. The common objective is to set up the initial state reducing to minimum any source of noise which tends to perturb the relaxation process of the concentration gradient. In any case, the initial experimental state differs from the theoretical one, being a hard task to place two miscible liquids in a Heaviside step initial state. The gap between experimental observations and theoretical predictions systematically induces a noise on the measured value of the diffusion coefficient, and its significance depends on the way in which the interface is carried out.

In order to bypass this problem, Longsworth [5] has proposed modelling the initial experimental state on an initial mixing state and to extrapolate the zero time of the theoretical initial step by a fit on data distribution. The zero-time linear shift correction is then the time interval t_0 that must be added to the recorded time t in order to obtain the correct value D of the diffusion coefficient. The reference relation is: $D_t t = D(t + t_0)$ where D_t is the measured vale of the diffusion coefficient at time t. The underlying hypothesis of having the whole data set in the one-dimensional free diffusion regime is guaranteed by observing a straight line when plotting the measured values D_t as a function of $1/t$.

In optical correlation analysis techniques, it is not simple to determine if all measured values are in the diffusive regime in order to apply the zero-time correction. A linear shift of the initial time is sometimes assumed a priori in data analysis methods which involve time correlations between pairs of digital images of the cell as in optical methods developed to measure the refractive index variation with concentration [3,6–9]. Moreover, it takes a finite time δt_0 to place two fluids into contact to form the initial state, which also induces uncertainty on fixing the experimental zero time on a reference frame, therefore, δt_0 should be held as low as possible. By using fluid injection procedures a low value of δt_0 might induce larger noise fluctuations on the interfacial region of the two liquid mixtures and longer transient. Longsworth [5] has also warned that when the boundary between solution and solvent is perturbed over the period of time during which it is being set up no simple linear zero-time correction might be applied. In this paper we report the result of a data analysis investigation developed to observe the relaxation

* e-mail: cinzia.deleo@univaq.it

process of the concentration gradient in time correlation data analysis. We consider the diffusion of 1.75 M NaCl (moles l^{-1}) aqueous solution in pure water while it is undergoing free diffusion in a cell filled through injection. By using digital speckle photography technique [10] we observe the dynamics of speckled patterns generated by a laser light beam which is bent when it passes through the cell. Speckle displacements are then measured in the time correlation mode developed by the particle image velocimetry (PIV) techniques [11]. The method applied in data analysis is the following: the correlation function is analysed assuming that the diffusion coefficient is related to time. This means that for each couple of images analysed two values of the diffusion coefficient are obtained. These vales are then used to observe the development of the process of diffusion in relation to time. We find a noise-to-signal ratio which decays faster than expected in the case of noise modelled on a linear shift of the zero-time but with a long relaxation time, much greater than the injection time, $\tau >> \delta t_0$. We get the diffusion coefficient corresponding to the unperturbed free diffusion limit.

2 Theoretical background

Emerging from a point on the exit face of a diffusion cell, a light ray has travelled along a path inside the diffusing medium which depends on the optical properties of the material. In a refractive index field it is described by the ray equation [12]:

$$\frac{d}{ds}\left(n\frac{dr}{ds}\right) = \nabla n, \tag{1}$$

where r is the vector position of a point situated on the ray path, s is a curvilinear abscissa. In a one-dimensional diffusion process the refractive index is a function of only one spatial variable, $n = n(y, t)$, and the two-dimensional trajectory of a light ray propagating along the z-axis is given, in paraxial approximation, by solving the system of differential equations:

$$\frac{d}{ds}\left(n\frac{dz}{ds}\right) = 0, \tag{2}$$

$$\frac{d}{ds}\left(n\frac{\mathrm{d}y}{ds}\right) = \frac{dn}{\mathrm{d}y}, \tag{3}$$

with $ds = \sqrt{(dz)^2 + (dy)^2}$ the arc-length element of the ray path. The resulting equation is then:

$$\frac{d^2y}{dz^2} = \frac{1}{2\gamma^2}\frac{dn^2}{\mathrm{d}y}, \tag{4}$$

where $\gamma = n\ dz/ds = n\cos\varphi$ is constant on the path of the ray, φ is the angle that the light ray makes with the z-axis. A binary system of two liquid mixtures, solution and solvent, initially separated at $y = y_0$, in a column with rectangular cross section, evolves following Fick's second law. The refractive index field of dilute solutions ia a linear function of concentration. Thus, for the given initial and boundary conditions it is expressed by [13]:

$$n(y,t) = n_m - \frac{\Delta n_o}{2} erf\left(\frac{y - y_0}{2\sqrt{Dt}}\right), \tag{5}$$

where D is the diffusion coefficient, n_m the refractive index of the fluid at the end of the diffusion process, and Δn_o is the initial difference between the refractive index of the two liquid mixtures. The initial $t = 0$ state corresponds to a sharp gradient expressed by the Heaviside step function with the solution in the region $y - y_0 < 0$. When $\Delta n_o/2n_m << 1$, one gets from equation (4):

$$\frac{d^2y}{dz^2} \simeq \frac{n_m}{\gamma^2}\frac{dn}{\mathrm{d}y}, \tag{6}$$

while the refractive index gradient, from equation (5), has a Gaussian distribution,

$$\frac{dn}{\mathrm{d}y} = -\frac{\Delta n_o}{\sqrt{4\pi Dt}}\exp\left[-\frac{(y - y_0)^2}{4Dt}\right], \tag{7}$$

and, therefore, equation (6) does not have an analytical solution. For smooth relaxation, the refractive index and its gradient are fairly constant along the path of the ray. The angle of refraction of a ray passing through a diffusion cell of thickness ℓ is

$$\phi_\ell = \frac{\mathrm{d}y}{dz}\Big|_{z=\ell} \simeq \frac{1}{n_m}\frac{dn}{\mathrm{d}y}\ell. \tag{8}$$

The relative displacement d between the positions y_v of the exit rays, at two instants in time t_1 and t_2, is estimated as [14,15]:

$$d = y_v(t_2) - y_v(t_1) = \left(\frac{dn}{\mathrm{d}y}\Big|_{t_2} - \frac{dn}{\mathrm{d}y}\Big|_{t_1}\right)\frac{\ell^2}{n_m}. \tag{9}$$

Figure 1 reports the profiles of two exit rays as a function of the position y along the cell. They have been obtained solving numerically equation (6) using a fourth-order-Runge–Kutta method [16] for $\Delta n_o/n_m = 1.3 \cdot 10^{-2}$, at the two instants in times $t_1 = 35$ min and $t_2 = 75$ min, in a diffusion cell of thickness $\ell = 10$ cm with a diffusion constant $D = 1.54 \cdot 10^{-9} \mathrm{m}^2/\mathrm{s}$.

The profile of the relative displacement d has two principal characteristics: the principal change of the concentration gradient at the diffusing interface $y = y_0$,

$$h = \frac{\Delta n_o}{n_m}\frac{\ell^2}{\sqrt{4\pi D}}\left(\frac{1}{\sqrt{t_2}} - \frac{1}{\sqrt{t_1}}\right), \tag{10}$$

and the relative distance w between the two turning points, which are related to the maximum value of the concentration difference,

$$w = \sqrt{\frac{8D\ln(t_2/t_1)}{1/t_1 - 1/t_2}}. \tag{11}$$

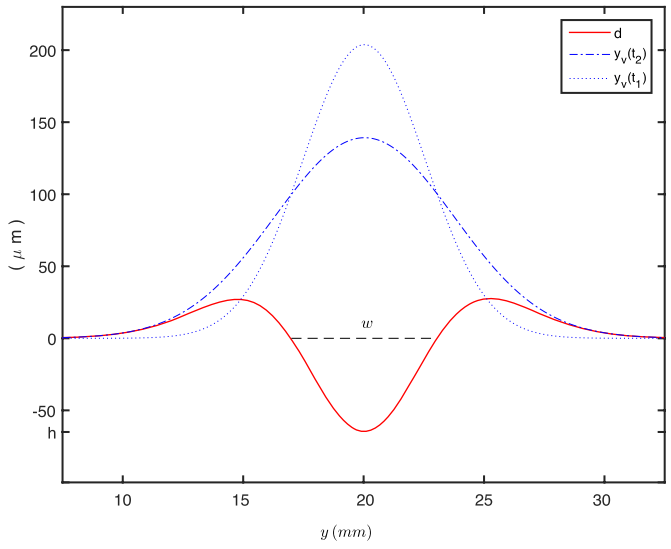

Fig. 1. Absolute and relative profiles of the light ray displacement y_v observed from the image point y of the cell at the times $t_1 = 35$ min and $t_2 = 75$ min in a diffusion cell with thickness $l = 1.0$ cm and diffusion coefficient $D = 1.54 \times 10^{-9}$ m^2/s. The relative profile is $d = y_v(t_2) - y_v(t_1)$.

These two points are situated in a symmetrical position in relation to the position $y = y_0$ of the interface.

3 Experimental set-up

Figure 2 shows a schematic drawing of the set-up. We use a classical spectrophotometric glass cell of internal dimensions 10 mm × 45 mm and a path length of $\ell = 10$ mm along the optical z-axis. The light source is a laser diode beam of wavelength 638.5 nm and maximal power of 5 mW (Lasiris by Stocker Yale). The laser beam is expanded and then collimated to illuminate the cell. A ground glass diffuser is placed at the laser entrance surface of the cell, then the scattered light generates a speckled pattern which is sensitive to the refractive index changes of the medium through which the light travels [17–19]. Speckled fields are then recorded through a lens on the matrix of the CCD camera Silicon Video 9T001C of 2048 × 1536 resolution with a pixel area size of 3.2 × 3.2 μm. A TEC-55 55 mm F/2.8 Telecentric Computar Lens reduces the viewing angle error and magnification error providing good resolution and contrast. The speckled pattern visibility and the spatial resolution are optimized for an average speckle diameter of 4 pixels, relative to the pixel size in the camera, and an aperture of $f/8$ of the lens [20].

The measurements are performed observing the diffusion of a 1.75 M(moles l^{-1}) solution of NaCl in pure water at $T = 26$ °C. Room temperature is controlled by the air condition system of the laboratory, while the air temperature is confirmed near the cell.

The refractive index increases linearly with the concentration in diluted aqueous solutions with the specific refractive index increment $v = 1.70 \cdot 10^{-1}$ ml/g for the wavelength 638.5 nm of the beam light, as extrapolated from data in the literature [21]. Thus, the refractive ratio for the binary mixtures is $\Delta n_o / n_m = \nu \Delta c / (n_o + \nu\ c_m) = 1.301 \cdot 10^{-2}$, where Δc is the initial concentration difference between the solution of NaCl and water, c_m is their average value and $n_0 = 1.331$ the refractive index of water [22].

The diffusion cell is first half filled with the solvent, pure water, and then the NaCl aqueous solution is slowly injected from the bottom using a capillary tube. Both solution and solvent are allowed to equilibrate at the room temperature before they are injected into the cell. At the end of the injection process, which takes a time interval $\delta t_o \sim 40s$, a sequence of single exposure image are acquired by the CCD camera for eighty minutes of working camera. Then, pairs of successive image frames are processed off-line by means of image processing analysis based on the cross-correlation technique used in PIV [23]. In this way we measure the speckle displacement related to the change of the refractive index gradient that takes place during the time interval separating the two recorded images.

Speckle displacements are statistically evaluated by correlating speckles contained within sub-images, the interrogation windows, placed at the same location of the two successive recorded images. Data analysis is performed using the adaptive cross-correlation algorithm developed by Astarita and his group [24–27], which is based on recursive correlation processing techniques to iteratively arrive at the local displacement, decreasing the interrogation window size during a multipass approach. The final interrogation window size is set to $L_y \times L_x = 10 \times 50$ *pixel* to obtain a better resolution in the direction of the diffusion and to have about 30 speckles as statistical sample to reduce the uncertainty of the measurement result. The cross-correlation procedure results in a signal peak on the correlation plane, which is a 2-dimensional pixel vector shift. The signal component along the diffusion direction y is then set equivalent to the displacement d of equation (9) by the optical magnification of the camera. A schematic graph of the imaging setup in PIV is given in Figure 3. The camera calibration gives one pixel corresponding to 12.57 μm in the diffusion cell. Ten pairs of final windows, along the horizontal direction x, are used for the ensemble averaging to get the resulting value.

4 Principles of measurements

An ideal one-dimensional free diffusion process starts with two miscible liquids, solution and solvent, initially separated by a sharp horizontal surface $y = y_0$ at the initial time $t = 0$. The variance of the refractive index gradient profile, in equation (7), spreads from the diffusion boundary proportionally to the elapsed time as $\sigma_t^2 = 2Dt$.

Real diffusion experiments set up the interface between the two liquids mixtures by a procedure which takes a finite time and blurs the diffusion boundary from the ideal sharp boundary assumed in the theory, so that the measured values of the diffusion coefficient drift with time.

The simplest case is when the drift of the diffusion coefficient can be modelled assuming a linear zero-time shift t_0 from the time $t = 0$ the boundary is experimentally formed. This effect has been shown by Longsworth [5] by

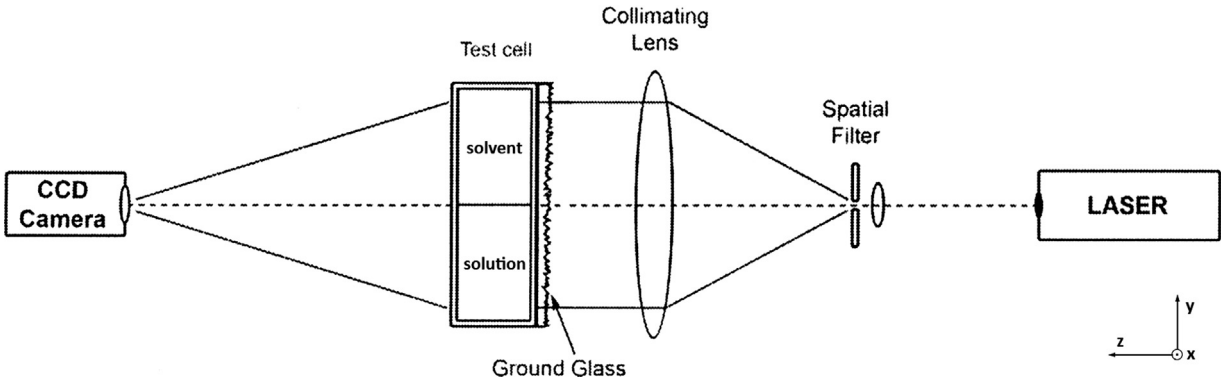

Fig. 2. Experimental set-up for digital speckle photography.

using a Gouy interferometer and two dilute electrolyte solutions set up in a Lamm diaphragm cell. The zero time correction is obtained first by measuring the downward displacement of the most deflected ray light as function of time, which is proportional to the maximum height $H = \Delta n_0/\sqrt{4\pi D(t-t_0)}$ of the refractive index gradient profile, and then extrapolating linearly to $1/H^2 = 0$, which gives the exact zero time t_0 of the process. The zero time is usually located at an earlier time from the time $t = 0$ when the boundary is set up, being related to the thickness $\lambda \sim \sqrt{Dt_0}$ of the blurred initial boundary in the diffusion cell. Thus, a constant increment t_0 must be added to the observed time t to obtain the corrected value D of the diffusion coefficient. The drift with time induced on the measured diffusion coefficient in the absence of time correction, is then

$$\frac{\Delta D_H}{D} \sim \frac{t_0}{t} \tag{12}$$

with $\Delta D_H = D_H - D$ where D_H is the diffusion coefficient measured at time t. If it is not observed and corrected, this effect results in an over estimation of the diffusion coefficient value.

In data analysis methods which involve temporal correlation between times $t_1 = t$ and $t_2 = t + \Delta t$, the drift with time induced on the measured values depends on the method chosen for the estimation of the diffusion coefficient. For example, if the principal relative change h of the refractive index gradient in equation (10) is detected then this is:

$$h(t, t+\Delta t, D_h) = h(t+t_0, t+t_0+\Delta t, D),$$

from which follows

$$\frac{\Delta D_h}{D} \sim \left(\frac{1/\sqrt{t} - 1/\sqrt{t+\Delta t}}{1/\sqrt{t+t_0} - 1/\sqrt{t+t_0+\Delta t}}\right)^2 - 1, \tag{13}$$

with $\Delta D_h = D_h - D$, where D_h is now an average value in the time interval from t to t to $t+\Delta t$, at $y = y_0$. However, considering the relative distance w in equation (11) this is:

$$w(t, t+\Delta t, D_w) = w(t+t_0, t+t_0+\Delta t, D),$$

from which follows

$$\frac{\Delta D_w}{D} \sim \frac{(t+t_0)(t+t_0+\Delta t)}{t(t+\Delta t)} \frac{\ln[1+\Delta t/(t+t_0)]}{\ln(1+\Delta t/t)} - 1, \tag{14}$$

with $\Delta D_w = D_w - D$, where D_w is now an average value in the time interval from t to $t+\Delta t$ and in the range $y = y_0 \pm w/2$. In both cases, the underlying assumption of an ideal one-dimensional free diffusion regime is not easy to confirm from data distributions because now the zero-time of the diffusion process can not be linearly extrapolated from data.

In measurements which involve Gaussian refractive index gradient profiles a noise can be modelled by adding a noise variance term σ_n^2. Thus, at the time t, the variance of the dynamic process is $\sigma_t^2 = 2D_t t = 2Dt + \sigma_n^2$. The measured value D_t is scattered by time as:

$$D_t = D + \sigma_n^2/2t. \tag{15}$$

If the diffusion process evolves unperturbed then the noise variance σ_n^2 is expected to be constant over time. This is equivalent to having a linear zero time shift $t_0 = \sigma_n^2/2D$ in the measured time t. In order to separate signal from noise we have extracted the temporal behaviour of D_t in time correlation analysis. The relative displacement profile d is fitted, through the least-square method [28], with the diffusion coefficient D_1 at $t = t_1$ and D_2 at $t = t_2$ as free parameters:

$$d = \frac{\Delta n_o \ell^2}{2n_m\sqrt{\pi}} \left[\frac{1}{\sqrt{D_2 t_2}} \exp\left(-\frac{y^2}{4D_2 t_2}\right) - \frac{1}{\sqrt{D_1 t_1}} \exp\left(-\frac{y^2}{4D_1 t_1}\right)\right]. \tag{16}$$

The central position, fixed at $y_0 = 0$, had been previously found by using a polynomial fit in order to detect the position of the principal change of the data profile. The spatial interval used for fitting is $[-7\text{mm}, 7\text{mm}]$ in order to cut off the tail of the profile at the lower and the upper range avoiding board effects. Moreover, this interval always encompasses the relative distance w between the two turning points in equation (16), which

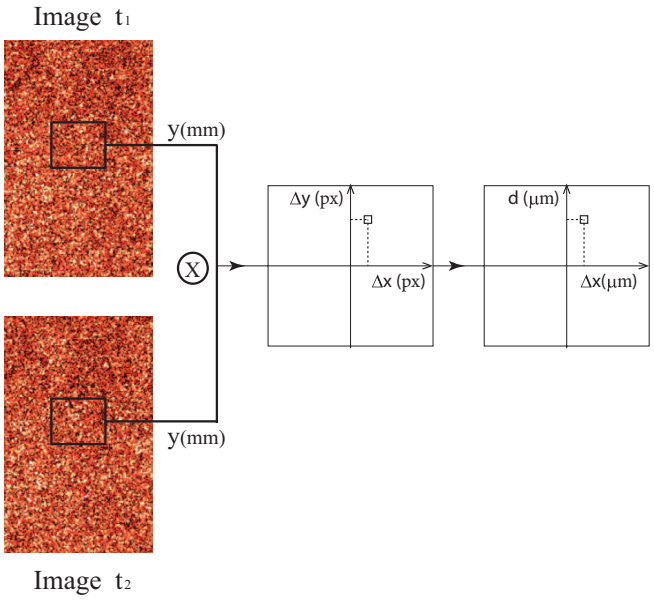

Fig. 3. Schematic representation of the imaging setup in PIV. The position of the cross-correlation peak gives the displacement.

is expressed as

$$w = \sqrt{\frac{8\ln(D_2t_2/D_1t_1)}{(D_1t_1)^{-1} - (D_2t_2)^{-1}}}. \tag{17}$$

Figure 4 shows a comparison between experimental data and the model after fitting. Table 1 reports the values of diffusion coefficient obtained for different pairs of times t_1 and t_2. The fitting procedure also returns the values of the diffusion coefficient in the two regions of the cell which are separated by the interface at $y_0 = 0$. These are labelled D^+ and D^- for positive and negative values of y, respectively. The values obtained show that an asymmetry is present in the Gaussian distribution of the refractive index gradient in equation (7). The result is a systematic shift, δ^+ and δ^-, of the position of the two turning points which are no longer in a symmetrical position with respect to the interface. In each region, a small change $\varepsilon_t^{\pm} = D_t^{\pm} - D_t$ of the diffusion coefficient at time t is related to the relative change $\delta^{\pm}$ of the position of the two turning points of equation (16) as

$$\delta^{\pm} = \sum_{t=1,2} \frac{1}{2}\frac{\partial w}{\partial D_t}\varepsilon_t^{\pm} = \frac{2}{w[(D_1t_1)^{-1} - (D_2t_2)^{-1}]} \left[\frac{D_1^{\pm} - D_1}{D_1}(\zeta D_2t_2 - 1) + \frac{D_2 - D_2^{\pm}}{D_2}(\zeta D_1t_1 - 1)\right], \tag{18}$$

where $\zeta = (D_2t_2 - D_1t_1)^{-1}\ln(D_2t_2/D_1t_1)$

In the low concentration region, $y > 0$, we observe $D_1^+ > D_1$ and $D_2^+ < D_2$, which both give $\delta^+ > 0$. Instead, the opposite behaviour is detected in the high concentration region, $y < 0$, where $D_1^- < D_1$ and $D_2^- > D_2$ with $\delta^- \simeq -\delta^+$. Table 1 depicts evaluated $\delta^{\pm}$ values for different pairs of times t_1 and t_2.

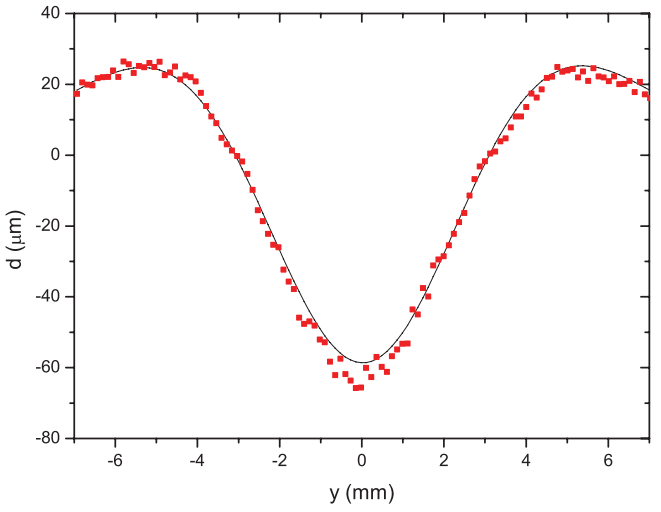

Fig. 4. Experimental data (squares) obtained for diffusion of NaCl solution in pure water with $t_1 = 35$ min and $t_2 = 75$ min. Solid line is the least square best fit using equation (16).

The intensity of $\varepsilon_t^{\pm}$ decreases with time. This suggests that after sufficiently long time the refractive index gradient profile will converge to the Gaussian profile of the unperturbed diffusion process.

To observe the dynamics of the diffusion process, the data in the Table 1 are plotted as a function of time.

Figure 5 shows the mean value of D_t as function of time, the uncertainty is set equal to the changes $\varepsilon^{\pm}$ detected in the two regions $y > 0$ and $y < 0$. This plot shows that the rate of decay of D_t is faster than that expected assuming a constant noise variance term σ_n^2 in equation (15). Therefore, it might be connected to a more complex noise dynamics induced during the injection of fluid in the cell, assuming the diffusion coefficient is independent of concentration.

Fluid injected into the cell can generate long range components of noise, varying temporally and spatially, as a consequence of initial macroscopic chaotic environmental fluctuations around the interfacial region and their subsequent decay bounded by gravity and the finite dimensions of the cross section of the cell. These perturbations are expected to die away through a homogenization process relaxing toward the dominant dynamic process in the cell. The noise variance σ_n^2 is then expected to be time correlated and its decay rate characterizes the fluctuating field [29–31]. As a rough estimation, we fit the data in Figure 5 assuming an exponential decaying mode of the noise variance, $\sigma_n^2 = \lambda^2\exp(-t/\tau)$, with λ related to the initial contour domain of the noise field and τ the mean life time of the decaying process. We model the noise dynamics on the time scale of the diffusion with $\lambda = \sqrt{2D\tau}$ the dominant wavelength of the noise field. This gives:

$$D_t = D\left[1 + \frac{\tau\exp(-t/\tau)}{t}\right], \tag{19}$$

where the diffusion coefficient D and the noise life time τ are the fitting parameters. The weighted least square fitting

Table 1. Diffusivity values D at times t_1 and t_2 and relative displacements of the two turning points, δ^+ and δ^-, by equation (18). D^+ and D^- are obtained by fitting through equation (16) only negative and positive y values.

t_1 (min)	D_1	D_1^+ (10^{-9} m/s^2)	D_1^-	t_2 (min)	D_2	D_2^+ (10^{-9} m/s^2)	D_2^-	δ^+ (%)	δ^-
25	1.759	1.794	1.724	50	1.559	1.540	1.580	0.27	−0.24
25	1.716	1.766	1.665	55	1.541	1.524	1.560	0.57	−0.55
30	1.645	1.670	1.621	60	1.570	1.550	1.590	0.14	−0.12
30	1.650	1.670	1.630	65	1.553	1.539	1.567	0.14	−0.14
30	1.665	1.700	1.630	70	1.540	1.530	1.550	0.45	−0.45
35	1.591	1.619	1.561	60	1.524	1.517	1.531	0.37	−0.40
35	1.612	1.640	1.583	65	1.535	1.525	1.545	0.33	−0.34
35	1.635	1.670	1.600	70	1.550	1.540	1.560	0.74	−0.74
35	1.633	1.662	1.602	75	1.540	1.530	1.550	0.35	−0.39
40	1.585	1.611	1.559	80	1.542	1.534	1.550	0.34	−0.34
45	1.553	1.572	1.533	80	1.543	1.535	1.553	0.22	−0.21

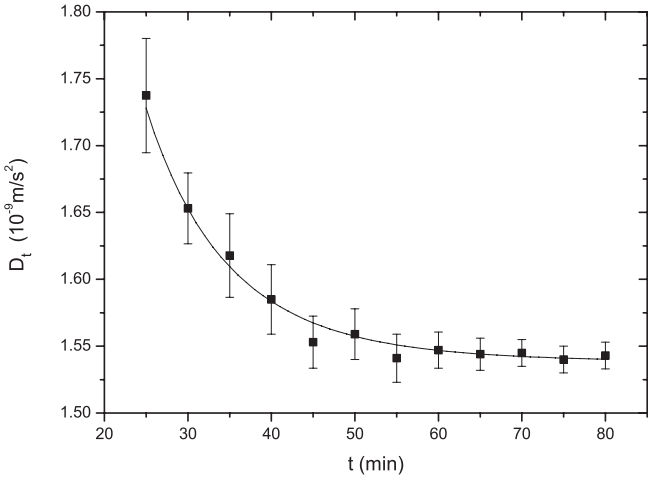

Fig. 5. The diffusivity D_t as function of time. Solid line is the weighted least square best fit, using equation (19).

technique is now performed to obtain the corresponding parameter values with the weights given by the uncertainty on D_t in order to take into account the different impact of noise on measurements.

The estimated diffusion coefficient, at a confidence level of 95%, is $D = (1.539 \pm 0.013) \cdot 10^{-9}\mathrm{m}^2/\mathrm{s}$. The mean life time of the decaying noise field is $\tau = (15 \pm 2)$ min, which is much greater than the injection time $\delta t_0 = 0.67$ min, and could be considered as the timescale crossover to the unperturbed free diffusion regime. The dimension of our sample, the data collected up to time $t = 80$ min, is not large enough to be also sensitive to the zero-time correction in the unperturbed free regime.

5 Conclusion

We propose to observe the effect of noise that is inevitably generated by the interfacing of two liquids when they are placed in a diffusion cell. This procedure generates a systematic error in the value of the diffusion coefficient, and its significance depends on the way in which the interface is carried out. In the case studied the diffusion cell is first half filled with the solvent, pure water, and then NaCl aqueous solution, is slowly injected from the bottom using a capillary tube.

The data analysis which we have implemented permits us to evaluate the diffusion coefficient in function of time when pairs of successive images of the diffusing cell are analysed using optical correlation technique. The values of the diffusion coefficient obtained are reported in Table 1. If any correction is made on these values the result is expressed by the average and the standard deviation: $D = (1.593 \pm 0.064) \cdot 10^{-9}\mathrm{m}^2/\mathrm{s}$. This result can be compared with that obtained by Riquelme et al. [32]. The authors of this work carry out a series of measurements through optical correlation in the same test conditions as us, and they then analyse them using two different techniques. However, they never correct the diffusion coefficient value, which is therefore expressed as the average value of the recorded measurements. Their results are: $D = (1.587 \pm 0.05) \cdot 10^{-9}\mathrm{m}^2/\mathrm{s}$ and $D = (1.602 \pm 0.05) \cdot 10^{-9}\mathrm{m}^2/\mathrm{s}$. Both are in agreement with the behaviour of the mean value and the standard deviation which we obtain.

Moreover, the analysis we have carried out allows us also to observe the progress of the diffusion process, plotting the same data shown in Table 1 as a function of time. Figure 5 shows the presence of noise that can not be interpreted as a zero-time linear shift from the time the boundary is formed but as a time correlated noise. Thus, if the data are analysed so as to separate the signal from the noise, then a value which is lower than the previous value of the diffusion coefficient is obtained: $D = (1.539 \pm 0.013) \cdot 10^{-9}\mathrm{m}^2/\mathrm{s}$. This new value is within the range of the expected values $[1.522\ ,\ 1.553] \cdot 10^{-9}\mathrm{m}^2/\mathrm{s}$, as reported by Riquelme et al. [32]. This interval is wide and also includes the extrapolated values that were obtained through measurements using other methods than optic methods [33].

Authors contribution statement

All the authors were involved in the preparation of the manuscript. All the authors have read and approved the final manuscript.

References

1. D. Ambrosini, D. Paoletti, N. Rashidnia, Opt. Lasers Eng. **46**, 852 (2008)
2. R.H. Stokes, J. Am. Chem. Soc. **72**, 763 (1950)
3. N. Bochner, J. Pipman, J. Phys. D Appl. Phys. **9**, 1825 (1976)
4. L. Gabelmann-Gray, H. Fenichel, Appl. Opt. **18**, 343 (1976)
5. L. Longsworth, J. Am. Chem. Soc. **69**, 2510 (1947)
6. A. Mialdun, V. Shevtsova, J. Chem. Phys. **134**, 044524 (2011)
7. A. Mialdun, V. Sechenyh, J.C. Legros, J.M. Ortz de Zárate, V. Shevtsova, J. Chem. Phys. **134**, 104903 (2013)
8. M.G. He, S. Zhang, Y. Zhang, S.G. Peng, Opt. Express **23**, 10884 (2015)
9. S. Zhang, M. He, Y. Zhang, S. Peng, X. He, Appl. Opt. **54**, 9127 (2015)
10. N.A. Fomin, *Speckle Photography for Fluid Mechanics Measurements* (Springer-Verlag, Berlin, 1998)
11. J. Westerweel, R.J. Adrian, *Particle Image Velocimetry* (Cambridge University Press, New York, 2011)
12. V. Lakshminarayanan, A. Ghatak, K. Thyagarajan, *Lagrangian Optics* (Springer Science, New York, 2002)
13. J. Crank, *The Mathematics of Diffusion* (Oxford University Press, New York, 1975)
14. G. Schirripa Spagnolo, D. Ambrosini, A. Ponticiello, D. Paoletti, J. Phys. III France **6**, 1117 (1996)
15. D. Ambrosini, D. Paoletti, A. Ponticiello, G. Schirripa Spagnolo, Opt. Lasers Eng. **37**, 341 (2002)
16. E. Hairer, C. Lubich, G. Wanner, *Geometric Numerical Integration* (Springer-Verlag, Berlin, 2006)
17. U. Köpf, Opt. Commun. **5**, 347 (1972)
18. D. Paoletti, G. Schirripa Spagnolo, D. Ambrosini, J. Phys. III France **2**, 1835 (1992)
19. G. Schirripa Spagnolo, D. Ambrosini, D. Paoletti, Eur. Phys. J. AP **6**, 281 (1999)
20. J.W. Goodman, *Speckle Phenomena in Optics: Theory and Applications* (Roberts and Co., Englewood, Colorado, 2007)
21. A. Kruis, Z. Physik. Chem. **34**, 13 (1936)
22. L.W. Tilton, J.K. Taylor, J. Res. Natl. Bur. Stand. **20**, 419 (1938)
23. R.D. Keane, R.J. Adrian, Appl. Sci. Res. **49**, 191 (1992)
24. T. Astarita, G. Cardone, Exp. Fluids **38**, 233 (2005)
25. T. Astarita, Exp. Fluids **40**, 977 (2006)
26. T. Astarita, Exp. Fluids **45**, 257 (2008)
27. F. Avallone, S. Discetti, T. Astarita, G. Cardone, Exp. Fluids **56**, 1 (2015)
28. G. Cowan, *Statistical Data Analysis* (Oxford University Press, New York, 1998)
29. J. Ottino, *The Kinematics of Mixing: Stretching, Chaos, and Transport* (Cambridge University Press, Cambridge, 1989)
30. V. Toussaint, P. Carriere, J. Scott, J.-N. Gence, Phys. Fluids **12**, 2834 (2000)
31. W. Liu, G. Haller, Phys. D **188**, 1 (2004)
32. R. Riquelme, I. Lira, C. Perez-Lopez, J.A. Rayas, R. Rodriguez-Vera, J. Phys. D Appl. Phys. **40**, 2769 (2007)
33. V.M.M. Lobo, Pure Appl. Chem. **65**, 2613 (1993)

Cite this article as: Cinzia De Leo, Domenica Paoletti, Dario Ambrosini, Effect of noise on measurements of diffusivity in transparent liquid mixtures by digital speckle photography, Eur. Phys. J. Appl. Phys. **82**, 30501 (2018)